Multifaceted Resistance of Gliomas to Temozolomide[1]

Dora B. Bocangel, Sydney Finkelstein, S. Clifford Schold, Kishor K. Bhakat, Sankar Mitra, and Demetrius M. Kokkinakis[2]

Department of Pathology, The University of Pittsburgh Cancer Institute, Pittsburgh, Pennsylvania 15261 [S. F., S. C. S., D. M. K.], and The University of Texas Medical Branch at Galveston, Galveston, Texas 77555 [D. B. B., K. K. B., S. M.]

ABSTRACT

***Purpose and Experimental Design*: The contributions of O^6-methylguanine-DNA-methyltransferase (MGMT), p53 status, mismatch repair, and apoptotic response to the resistance of glial tumors to temozolomide (TMZ) were tested using seven established human glial tumor cell lines in culture and xenografts in athymic mice.**

***Results:* Resistance to TMZ was only marginally dependent on MGMT activity, because subtoxic doses of TMZ easily eliminated MGMT reserves for at least 18 h after treatment. Resistance to TMZ varied most notably with the p53 status of the tumor. Tumors with wild-type (wt) p53 and a functional p53 response to DNA damage (SWB40 and SWB61) were most sensitive. The p21-related cell cycle arrest was intimately linked to TMZ toxicity because tumors with wt p53 but lacking a robust increase in p21 protein level (D-54) were resistant to TMZ. In contrast, tumors with a dysfunctional p53 cycle and a weak cell cycle response to DNA damage (SWB39 and SWB77) were extremely unresponsive to treatment even with the aid of MGMT inactivators. Notable exceptions to the above were observed with the p53 mutated tumors SWB33 and SWB95, which were arrested by TMZ in G_1-S and consequently underwent apoptosis despite their failure to express p21.**

***Conclusions*: By testing a limited number of glial tumors in cell culture and also as xenografts, we have shown that mobilization of the p53 in response to TMZ damage is likely to induce a cell cycle arrest and apoptosis in glial tumors. Additional pathways linking cell cycle arrest and apoptosis contribute to the efficacy of TMZ against p53 mutated glial tumors. The unusual resistance of tumors, of which the cell cycle was not arrested in response to TMZ treatment, was associated with allelic losses during regrowth of treated tumors. Nevertheless such resistance was not related to dysfunctional mismatch repair.**

INTRODUCTION

The prognosis for 20,000 new cases of brain tumors per year in the United States alone is particularly abysmal. Median survival in patients with glioblastoma multiforme is less than a year even when treated with the most aggressive regimens of cytoreductive surgery, radiation, and chemotherapy (1). The propensity of individual neoplastic cells to migrate away from the primary brain tumor mass, along white matter pathways (2), renders treatments directed solely at that main tumor mass of palliative benefit only. To date, no treatment has been developed that can prevent residual neoplastic cells that remain viable after surgery and radiation therapy to proliferate and cause these tumors to recur. Alkylating drugs such as BCNU[3] and *N*-(2-chloroethyl)-*N′*-cyclohexyl-*N*-nitrosourea have been somewhat effective against anaplastic astrocytomas (3, 4), but their action is limited by the presence of mechanisms of resistance, one of the most prominent of which is the up-regulation of MGMT during neoplastic progression (5, 6). MGMT confers resistance in tumors to agents that exert their cytotoxic action via the formation of O^6-alkylguanine adducts that either form lethal double-strand cross-links (7), as is the case with bifunctional nitrosoureas [BCNU and *N*-(2-chloroethyl)-*N′*-cyclohexyl-*N*-nitrosourea], or initiate mismatch abortive repair and DNA fragmentation, which results in cell death, as is the case with TMZ, procarbazine, and other DNA methylating agents (8, 9). The involvement of MGMT in the resistance of brain tumors to DNA alkylating drugs has been demonstrated with the use of MGMT inactivators such as BG or dBG, which enhance the efficacy of a variety of DNA alkylating agents against brain tumor xenografts in mice (10–12). These advances have promoted the general notion that drugs that have been marginally active against brain tumors in the past could be successfully reintroduced in combination with MGMT inhibitors, and a number of clinical trials have been completed or are currently in progress to determine the feasibility of such a strategy (13–15). Unlike BCNU, the resistance to which tends to be linked mainly and directly to the expression of MGMT, the resistance of glial tumors to monofunctional alkylating agents seems to follow a more complex pattern than simple dependence on MGMT levels, and may be controlled by additional DNA repair processes, apoptotic pathways, or cell cycle check points. These processes may not be entirely independent. A correlation between wt-p53 suppression of MGMT transcription, and a related decrease in

Received 10/31/01; revised 4/3/02; accepted 4/18/02.

The costs of publication of this article were defrayed in part by the payment of page charges. This article must therefore be hereby marked *advertisement* in accordance with 18 U.S.C. Section 1734 solely to indicate this fact.

[1] Supported by National Cancer Institute Grants CA 57725, CA84461, and CA 78561.

[2] To whom requests for reprints should be addressed, at Department of Pathology, University of Pittsburgh Cancer Institute, Pittsburgh, PA 15261. Phone: (418) 648-9850; Fax: (412) 383-9822; E-mail: Kokkinakisdm@msx.upmc.edu.

[3] The abbreviations used are: BCNU, 1,3-bis(2-chloroethyl)-1-nitrosourea; MGMT, O^6-methylguanine-DNA methyltransferase; BG, O^6-benzylguanine; dBG, O^6-benzyl-2′-deoxyguanosine; MMR, mismatch repair; TMZ, temozolomide; wt, wild type; TUNEL, terminal deoxynucleotidyl transferase (Tdt)-mediated nick end labeling; TG, thioguanine.

Table 1 p53 reverse transcription-PCR primer sequence and description

RDL#	Base pair position	Primer length (mer)	Sequence	Product size (bp)
N5335	167	21	5′GACACGGTTCCCTGGATTGGC3′	
N5336	619	22	5′GCAAAACATCTTGTTGAGGGCA3′	452
N5337	537	22	5′GTTTCCGTCTGGGCTTCTTGCA3′	
N5338	904	21	5′GGTACAGATCAGAGCCAACCTC3′	367
N4433	813	20	5′ATTTGCGTGTGGAGATATTG3′	
N4434	1389	21	5′AGAAGATGGAGAATGTCAGATCT3′	598

resistance to chloroethylnitrosoureas has been reported (16); and in general, wt-*p53*-containing cell lines have lower MGMT levels than those in mutant p53-containing cells (17–19). Signaling between MMR and p53 has also been suggested (20). wt-p53 plays a key role in mediating cell death of tumor cells through DNA damage-induced activation of apoptotic mechanisms. Activation of Bax, DR5, and Fas/APO1 or by protein-protein interactions with key elements in DNA synthesis or repair facilitates apoptosis (21–23). *p53* can induce cell arrest (when the genome is damaged to a limited extent, providing time to repair the DNA) or it can trigger apoptosis when damage is too severe for repair (21–22). Inactivation of p53 during malignancy allows highly damaged cells to survive and to accumulate mutations, thus increasing their propagation to oncogenic transformation, and possible acquisition of additional resistance to cytotoxic agents, through selection of clones with inactivated cell cycle checkpoints. Given the role of p53 in cell cycle progression and survival, and its recently reported interactions with DNA repair pathways it is likely that p53 status could predict the outcome of treatment of certain types of tumors.

In this study we have examined seven high-grade glial tumors in terms of their resistance to TMZ both in cell culture and also in xenografts; their p53, MGMT, and MMR status; their cell cycle response to DNA damage; and their ability to undergo apoptosis in response to DNA damage. These systematic investigations have yielded several new pieces of information regarding mechanisms of resistance of glial tumors to methylating agents and are likely to set the stage for clinical trials using such agents in combination with procedures to overcome the nonresponsiveness of the cell cycle of the most resistant glial neoplasms to DNA damage (24).

MATERIALS AND METHODS

Chemicals. BG and dBG were synthesized and purified according to methods published previously (25, 26) and donated to us by Dr. Robert Moschel. TMZ was a gift by Schering-Plough Inc. (Madison, NJ).

Cell Culture and Treatment Conditions. All of the cell lines used in this study (SWB 33, 39, 40, 61, 77, 95, and D54) were derived from human high-grade gliomas. They were grown in 5% fetal bovine serum (Life Technologies, Inc., Gaithersburg, MD) in Eagle's minimum essential medium-α modification (Life Technologies, Inc.) supplemented with lysine, valine, methionine and leucine (100 μM each), nonessential amino acids (1:100 dilution of stock; Life Technologies, Inc.), 1 mM sodium pyruvate, 1 μM α-hydroxycobalamin, 10 μM folic acid, and 0.2 mg/ml gentamicin. LoVo cells were obtained from American Type Culture Collection, and grown in Ham's F12 medium containing 10% fetal bovine serum (Life Technologies, Inc.). All of the cells were grown at 37°C in 5% CO_2 and tested routinely for *Mycoplasma* contamination with Hoechst 33258 stain.

Animals/Tumors. Four-week-old BALB/c-*nu/nu* athymic mice were purchased from Harlan Labs (San Diego, CA). Mice were maintained under barrier conditions and given sterilized food (Harlan Teklad laboratory diet) and water. s.c. tumors grew on injection of 3 million cells/animal. Tumor xenografts D-54, SWB 33, SWB39, SWB40, SWB77, and SWB61 had MGMT activities of <10, 56, 10, 45, 75, and 16-fmol/mg protein, respectively, as determined by the biochemical assay (27). Respective mitotic indices in xenografts were 5.5, 5.7, 8.2, 12.1, 5.7, and 12.9 m/high powered field (×400).

Drug Doses. All of the treatments were administered i.p. BG was dissolved in 40% polyethylene glycol 400/60% PBS. The pH of the solvent was corrected to 7.0 before the addition of the drug. TMZ was dissolved in 100% DMSO. MGMT inhibitors were administered at volumes of 30 ml/m^2 and alkylating drugs at 20 ml/m^2. Drug doses were calculated as mg/m^2 using the formula: meters (m) = weight $(g)^{2/3} \times K \times 10^{-4}$, where K is 10.5 for mice (28). In animals of 20 ± 2 g used in this study, the weight (kg) of the animal is ~2.6 times the area surface (m^2).

Tumor Implantation and Treatment. Two hundred μL containing 3×10^6 cells of tumor cells in 5% serum medium were injected at the left flank of 6-week-old athymic mice weighing between 18 and 22 g. Visible tumors appeared in most of the animals within 3 weeks after implantation. The tumors were subsequently measured with calipers in two perpendicular dimensions, and their volumes were estimated using the formula $(\alpha^2 \times \beta)/2$, where α is the shorter and β the longer of the two dimensions. Treatment with TMZ in DMSO was administered i.p. to animals having tumors ranging between 325 and 375 mm^3. Animals were killed at 24 and 48 h after treatment with TMZ; the tumors were excised and processed for histology. Control animals bearing tumors were treated with DMSO and were killed at the same time intervals.

Immunohistochemistry and Immunocytochemistry. Immunoperoxidase staining for phosphorylated p53 and p21 were performed on formalin-fixed, paraffin-embedded tissue sections following the standard protocol recommended by the manufacturer (Cell Signaling Technologies). Briefly, 5-μm tissue sections mounted on Superfrost/Plus slides (Fisher), were deparaffinized, rehydrated, and incubated with 1.0% H_2O_2 in Tris-buffered saline to block endogenous peroxidase activity. Antigen unmasking was performed heating samples in sodium citrate buffer (10 mM sodium citrate, pH 6.0) 10 min, 100°C. Nonspecific protein binding was blocked by incubation in 5%

Table 2 The resistance of glioma cell lines to TMZ depends on MGMT

Cell line	MGMT	$IC_{50(10)}$ (TMZ)	$IC_{50(10)}$ (TMZ + BG)
SWB95	109[a]	100[b] (880)	50 (350)[c]
SWB77	75	350 (>1000)	300 (800)[c]
SWB33	56	75 (120)	54 (100)
SWB40	45	48 (80)	50 (100)
SWB39	10	125 (330)	110 (235)
SWB61	16	30 (50)	35 (50)
D54	5	96 (135)	87 (110)

[a] MGMT level (fmol/mg protein).
[b] μM.
[c] Statistically significant as compared to BG untreated (<0.05).

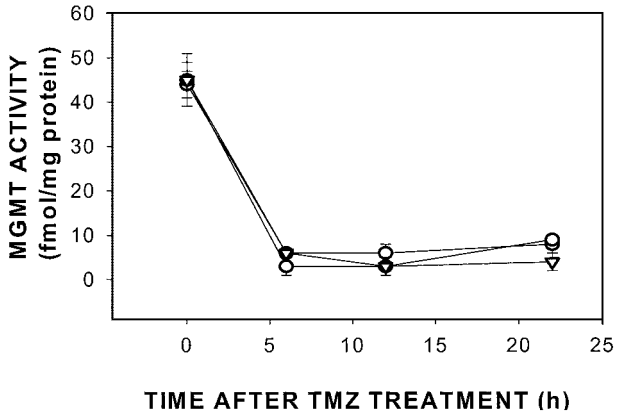

Fig. 1 Time course of depletion of MGMT activity in SWB40 tumor xenografts after treatment with 240 mg/m^2 TMZ (○), 180 mg/m^2 BG (●), or 250 mg/m^2 dBG (▽). Mean of three determination; *bars*, ±SD.

Table 3 p53 status of human glioma cell lines

Tumor	p53 pos.	Mutation codon[a]	Mutation	aa	wt
SWB77	215	72	CGC	Arg	
	714	238	TGG	Trp	Cys
SWB39	215	72	CGC	Arg	
	474	158	CCG	Pro	Arg
SWB33	215	72	CGC	Arg	
	725	242	TTC	Phe	Cys
SWB95	215	72	CGC	Arg	
	472	157	GTG	Val	Val
	638	213	CAA	Arg	Gln
	725	242	TTC	Phe	Cys
SWB61	215	72	CGC	Arg	
D54	215	72	CGC	Arg	
SWB40	215	72	CGC	Arg	

[a] p53 sequencing data.

horse serum in PBS [(pH 7.2–7.4) 10.4 mM Na_2HPO_4, 3.16 mM KH_2PO_4, and 123 mM NaCl]. Rabbit polyclonal (for p53) or monoclonal (for p21) IgG were applied to the sections and incubated (in blocking solution) overnight at 4°C. Serial sections of the tumor without primary antibody were used as negative control. After washing in PBS, the tumor sections were incubated in secondary antibody for 30 min at room temperature. The sections were washed again, treated with Elite ABC (Vectastain), washed, and developed with 3,3′-diaminobenzidine tetrahydrochloride (50 mg 3,3′-diaminobenzidine in 100 ml PBS and 150 μL of 3% H_2O_2). After rinsing in PBS, slides were dehydrated in graded alcohols, cleared in xylene, and permanently mounted. For immunocytochemistry, cells were grown on 1 mm coverslides (Corning) and, after drug treatment, fixed (freshly made 4% paraformaldehyde, 5% sucrose solution, in PBS), stained, and mounted (DAKO). Standard immunocytochemistry procedures were used. Briefly, nonspecific binding was blocked in incubating slides, in 5% normal goat serum in Tris buffered saline 0.05% Tween 20, 60 min at room temperature [50 mM Tris-HCl (pH 7.2–7.4)], 150 mM NaCl, and 0.05% Triton X-100]. The slides were then incubated in primary antibody diluted in blocking serum. A polyclonal (p53) rabbit antibody that recognizes (Serine-15) phosphorylated p53 (Cell Signaling Technology) was used to determine activated p53 protein. Alternatively, we also used a monoclonal rabbit (p21; Santa Cruz Biotech), and mouse (p53, DO-1; Santa Cruz Biotech) antibody. Cells were washed in TBST and then incubated with biotinylated secondary antibody for 60 min at room temperature. Cells were washed, and secondary antibody was detected using Streptavidin-linked Alexa 488 (Molecular Probes Inc.). Slides were then mounted (DAKO), images captured using a Nikon Eclipse-800 epifluorescent microscope and a couled monochrome CCD300T video camera from DAGE-MTI (Michigan City, IN), and analyzed using Metamorph imaging software (Universal Imaging Corp., Westchester, PA).

Clonogenic Survival Assays. Exponentially growing cells were seeded at a density of 250 to 300 cells/60-mm dish and left to attach for 24 h; then the cells were either pretreated with BG at 20 μM, TMZ (at specified concentrations), or mock-treated. For the BG colony-forming assays, cells were incubated for 2 h in serum containing medium with BG and then changed to serum free, TMZ containing medium for 30 min, then switched back to serum and BG containing medium. Twenty-four h afterward the cells were changed to BG free, serum-containing medium and left for 2 weeks to grow colonies, after which they were fixed and stained with a crystal violet/formalin solution, and counted. Cell survival is estimated from the number of colonies (defined as a cluster of >50 cells) formed and expressed as a percentage of the number of colonies in the control. Assays were set up in quadruplicate, and SDs were used in the calculations instead of SEs.

TUNEL Assays and Apoptotic Indices. Briefly, the cells were treated with TMZ, resuspended, fixed, and labeled (TUNEL assay; Boehringer Mannheim) according to the manufacturer's protocols at either 24 or 48 h after treatment with TMZ (100 μM). Apoptotic indexes were calculated scoring five randomly selected fields (number of cells counted over 400) and extrapolating the results to the number of apoptotic cells in 1000 cells.

Western Blots. Cells were lysed as described earlier (29), and protein concentration was determined using the Bradford Reagent (Bio-Rad); 20–30 μg protein was run on SDS-PAGE (10% for MMR proteins and 12% acrylamide for all of the others; acrylamide). Protein was then electroblotted to nitrocellulose membranes (40 V overnight at 4°C) in transfer buffer containing 25 mM

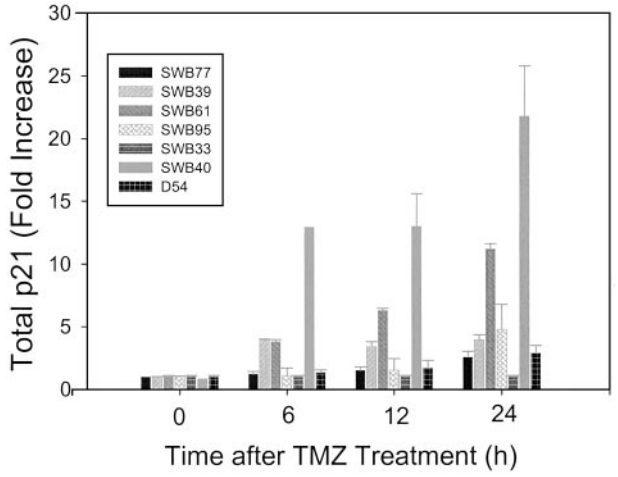

Fig. 2 Effect of TMZ on the expression of p21 in glioma cell lines. Glioma cell lines were exposed to TMZ (100 μM) for 1 h in serum-free conditions, after which cells were lysed, and proteins both in the nuclear and cytosolic fractions separated by SDS-PAGE and probed for expression of p21 as described in "Materials and Methods." Each lane was loaded with 30 μg protein. Blots were subsequently stripped and reprobed for β-actin to ensure equal loading and transfer. Values represent the means for three independent experiments performed in triplicate; *bars*, ±SD.

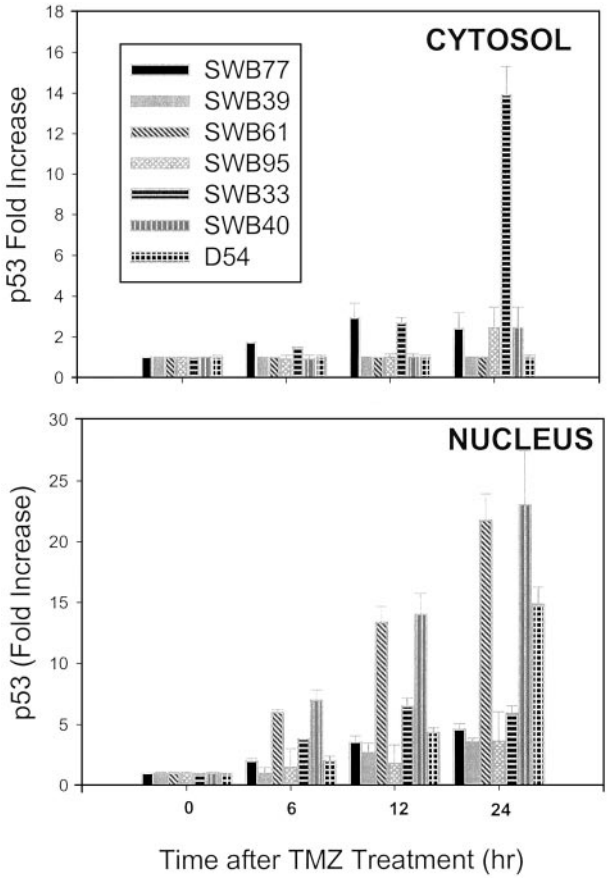

Fig. 3 Effect of TMZ on the expression and nuclear translocation of phosphorylated p53 in glioma cell lines. Glioma cell lines exposed to TMZ (100 μM) for 1 h in serum-free conditions, after which cells were lysed, proteins in the nuclear and cytosolic fraction separated by SDS-PAGE, and probed for expression of phosphorylated p53 as described in "Materials and Methods." Each lane was loaded with 30 μg protein. Blots were subsequently stripped and reprobed for β-actin to ensure equal loading and transfer. Values represent the means for three independent experiments performed in triplicate; *bars*, ±SD.

Tris-HCl, 129 mM glycine, and 20% methanol. Membranes were blocked in 5% milk in TBST, incubated in primary antibody (in TBST, 5% milk for 1 h at room temperature), rinsed, and incubated in horseradish peroxidase-conjugated secondary antibody (Amersham). Western blots were visualized using enhanced chemiluminescence (Amersham). Antibodies to p53 (DO-1), phosphorylated p53 (Cell Signal Technologies), p21 (Santa Cruz Biotechnologies), and β-actin (Sigma) were used at optimal titrations.

TG Assays. Clonogenic survival assays were set up with LoVo and glioma cell lines for TG (0.001–3 μg/ml). Briefly, cells were plated at low density (300 cells/60-mm dish) and allowed to attach for 24 h, then the cells were switched to medium containing the required amount of TG. The medium was changed every 3–4 days to replenish the treatments. Cells were harvested after 2 weeks, fixed, and stained with a crystal violet/formalin solution, and counted. Cell survival was estimated from the number of colonies formed, expressed as a percentage of the number of colonies in the control dishes. Assays were set up in quadruplicate, and SDs used instead of standard errors.

Sequencing of *p53* Gene in Tumor Lines. Total RNA was isolated from 70–80% confluent cells with RNAzol B (Tel-Test Inc.), and reverse-transcription PCR (GeneAmp RNA PCR kit; Perking Elmer) was performed using the following conditions (for cDNA: room temperature for 10 min, 37°C for 1 h, 90°C for 3 min, and 4°C for 5 min; PCR: 95°C for 2 min, 94°C for 30 s, 58°C for 50 s, and 72°C for 45 s, 37 cycles. Final elongation was done for 10 min at 72°C). Three sets of overlapping regions were sequenced (forward and reverse sequences); primers used are described in Table 1.

Genetic Analysis. Presence and extent of allelic loss and microsatellite instability were assessed by a broad panel of polymorphic microsatellites situated at the following genomic loci: 1p (D1S407, D1S1193, and MYCL), 9p21 (D9S251 and D9S254), 10q23 (D10S520 and D10S1173), 17p13 (D17S974, D17S1289, D17S1303, and TP53), and 19q (D19S400 and D19S559). DNA extracts from the xenografts used, under various treatment conditions, and also from human nonpolyposis colorectal cancers displaying microsatellite instability (positive controls), were PCR amplified across each microsatellite using flanking oligonucleotide primers bearing fluorescent labels for quantitative detection (GeneScan; Applied Biosystems). Nucleic acid amplification was performed according to manufacturer's instructions (GeneAmp kit; Perkin-Elmer-Cetus). The PCR products underwent capillary electrophoresis (ABI 310; Applied Biosystems) with quantitative determination of polymorphic alleles. Non-neoplastic tissue from the source of the cells was not available. Instead, the untreated cell line served as the starting point of the analysis with all of the microsatellites manifesting single alleles classified as noninformative for this

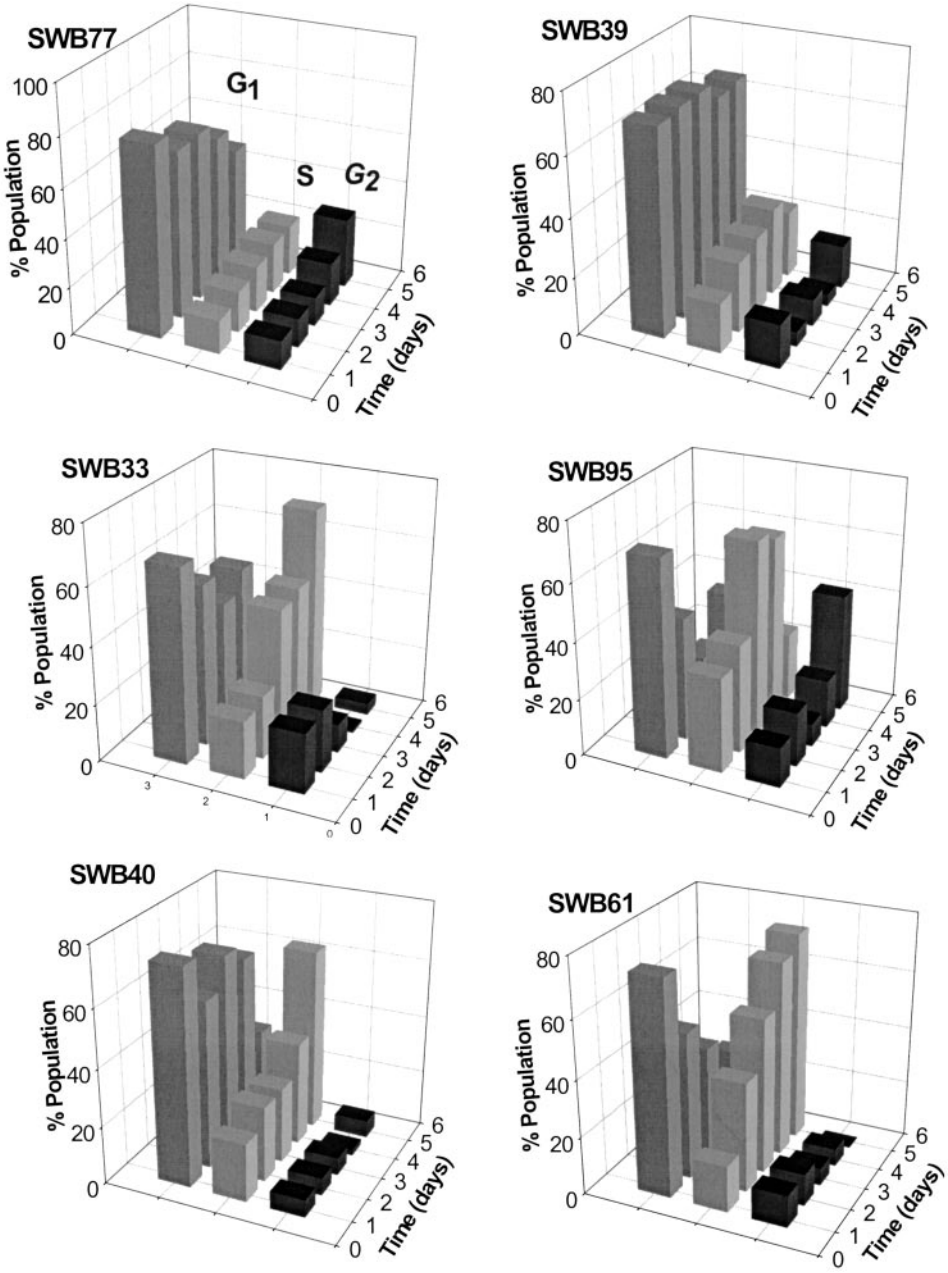

Fig. 4 Cell cycle distribution of glioma cell cultures treated with TMZ. Glioma cells were grown to 70% confluence treated with BG (20 μM) and TMZ (100 μM) harvested at the times indicated, stained for propidium iodide, and analyzed by flow cytometry. The results were analyzed by MODFIT LT statistics program (Verity Inc., Burlington, MA). The distribution of nuclei in G_1, S, and G_2 with various DNA contents is shown for SWB77, SWB39 (not responding, mut-p53), SWB33, SWB95 (responding, mut-p53), SWB40, and SWB61 (responding, wt-p53).

analysis. Allelic balance was determined to be present when the peak height ratio formed by dividing the longer allele by the shorter allele fell into the numerical range from 0.66 to 1.50. Low-level allelic loss was said to be present when the ratio was between 0.50 and 0.66 or 1.5 and 2.0. High-level allelic loss was assessed as being present when the allelic ratio fell below 0.50 or above 2.0. The closer the values approach 0 or infinity, the greater the degree of allelic imbalance. All of the analyses were performed in triplicate with the average taken for the three readings. Under these conditions, at least 50% of the cells contributing DNA to individual analyses would be required to have hemizygous loss for high-level allelic loss to be detected.

RESULTS

The resistance of glioma cell lines to TMZ and its correlation with levels of expression of MGMT is shown on Table 2. Unlike BCNU, the cytotoxicity of which closely parallels MGMT activity (30), there was not a clear correlation between MGMT activity and response to TMZ at the range of MGMT expressed by these cell lines and xenografts. For example, SWB77 was markedly more resistant than SWB95 despite a lower level of MGMT activity. Similarly, SWB33 and SWB40 showed different sensitivity to TMZ despite comparable levels of MGMT activity, and SWB39 was quite resistant despite a low level of MGMT activity.

Table 4 Effect of cell cycle arrest on apoptosis in glial cell tumor cells (*in vitro*)

Cell line	Agent[a]	Cell cycle arrest	Apoptotic index
wt p53			
SWB54	TMZ	+	55
SWB40	TMZ	+	89
SWB61	TMZ	+	126
Mutant p53			
SWB33	TMZ	+	43
SWB95	TMZ	+	91
SWB39	TMZ	−	29
SWB77	TMZ	−	18

[a] Toxicity assays were performed at 100 μM TMZ for all lines except for SWB77 and SWB95, which were treated with 200 μM TMZ. All cells were pretreated with BG to neutralize MGMT.

TMZ itself is quite effective in reducing MGMT activity levels below 10 fmol/mg protein (Fig. 1), so that moderate levels of MGMT activity in a tumor (<70 fmol/mg protein) are not playing an active role in the resistance of tumors to this agent (30). Clearly other resistance mechanisms are in play.

Table 3 shows the p53 status of the glial tumors used in this study. Three of the tumors had wtp53 sequence (SWB61, SWB40, and D54), whereas the other 4 had mutated p53 (SWB95, SWB77, SWB39, and SWB33). Although the susceptibility of SWB40 and SWB61, and the resistance of SWB77 and SWB39 to TMZ correlated with their p53 status, the mutational status in p53 alone did not determine the resistance of tumors to TMZ by itself. For example, the relative resistance of D-54 as compared with either SWB40 or SWB61 to TMZ was unexpected, because this tumor had no detectable MGMT and expressed wtp53. Its resistance could be associated to inefficient p21 induction after treatment with TMZ. In comparison, the sensitive tumor lines SWB61 and SWB40 showed a robust p21 induction in response to TMZ treatment (Fig. 2). Unlike tumors having wt p53, those with mutated p53 did not induce a higher level of p21 protein in response to TMZ treatment.

Expression of p21 succeeded the translocation of phosphorylated p53 to the nucleus. Nuclear translocation of p53 was robust in SWB61, SWB40, and to a lesser extent in D-54, whereas there was only marginal response in lines with mutated p53 sequences (Fig. 3). In SWB95, which had a mutated p53 sequence, the p53 was phosphorylated but did not show significant nuclear translocation. Despite the failure of p53-mutated tumors to phosphorylate p53, trigger induction of p21 protein level, and induce G_1-S arrest, the TMZ-induced DNA damage caused significant perturbations of cell cycle populations in all of the p53 mutant lines tested with the exception of SWB77 (Fig. 4). Although these perturbations were less persistent or pronounced than those seen in cells expressing wtp53, such as SWB61 and SWB40 (Fig. 4), it was evident that persistent cell cycle checkpoint arrests were also induced by mechanisms that were p53-independent in glial tumors.

The importance of cell cycle arrest in the effectiveness of treatment of glial tumors to TMZ is demonstrated in Table 4. The extent of TMZ-induced apoptosis during exponential growth of glial cells in culture was directly related to the extent of cell cycle arrest. The larger apoptotic indices were observed in SWB40 and SWB61, and SWB95 followed by SWB33. SWB77 and SWB 39 did not show significant apoptotic responses after exposure to TMZ whereas marked responses were observed in the p53-deficient lines SWB33 and SWB95 (Fig. 5). Thus, apoptosis was not necessarily associated with a w*tp53* sequence in glial tumors but rather with a functional mechanism to arrest the cell cycle in response to TMZ induced damage.

Correlations between the expression of p53/p21, cell cycle arrest, and apoptosis similar to those observed in culture also applied in xenografts 48 h after their treatment with TMZ. Expression of phosphorylated p53 and p21 was evident in SWB40, SWB61, and D-54, but not SWB77, 95, or 39 after a single injection of 400 mg/m^2 TMZ in mice bearing these tumor xenografts (Fig. 6). The correlation between apoptosis and glial tumor cells that undergo cell cycle arrest is also evident in comparisons between SWB95 and SWB77 (Table 5).

The apoptotic response of cells to TMZ treatment could be attributed to differences in MMR among the lines tested and possible greater MMR effectiveness in cell lines with wtp53 to restrict propagation through the cell cycle as long as O^6-methylguanine:thymine mismatches exist. A defective MMR could explain why the resistance of SWB77 to TMZ is only partially reversed by MGMT inhibition, as well as its poor apoptotic response, and the absence of G_2 cell cycle blocks to TMZ-induced damage. Thus, MMR was examined by direct measurement of MMR proteins (Table 6) and by the TG assay (Fig. 7) using LoVo, a MMR-deficient tumor line, as a control. Our results show the following. First, all of the brain tumor cell lines we tested, including SWB77, expressed similar levels of all of the key MMR proteins that characterize functional MMR. Second, SWB77 was as sensitive as SWB40 or SWB61 to TG and an order of magnitude less resistant than the MMR-defective LoVo. Finally, genetic analysis for presence and extent of allelic loss in cell lines assessed by a broad panel of polymorphic microsatellites indicated that treatment with TMZ does not result in microsatellite sequence slippage.

When allelic loss genotyping was performed on a broad panel of 13 microsatellites, only 4–5 markers were found to be informative in any given cell line consistent with a high degree of allelic loss already present in the untreated glioma lines used in this study. All of the informative markers in the untreated cell lines showed allelic balance of polymorphic alleles. After treatment with BG and TMZ, as reported previously (28), xenografts exhibited various degrees of allelic loss in informative markers. Noteworthy in this regard was the finding that all of the pretreatment informative markers developed various degrees of allelic imbalance indicating clonal expansion of glioma cells with greater genomic structural damage. Two patterns of acquired allelic loss were evident with respect to the manner in which individual cell lines responded to BG and TMZ treatment. In the first pattern, all of the informative markers showed only low-level allelic loss. This was true for the D-54, SWB40, and SWB61, and indicated significant admixture of nonmutated and mutated glioma cells in the tumors. In the second pattern of response, a very high degree of allelic imbalance was noted with near total replacement of pretreated xenografts with tumors showing allelic loss for all of the remaining markers. It is noteworthy that SWB77 xenografts regrown in animals treated with TMZ were entirely mutated (Table 7).

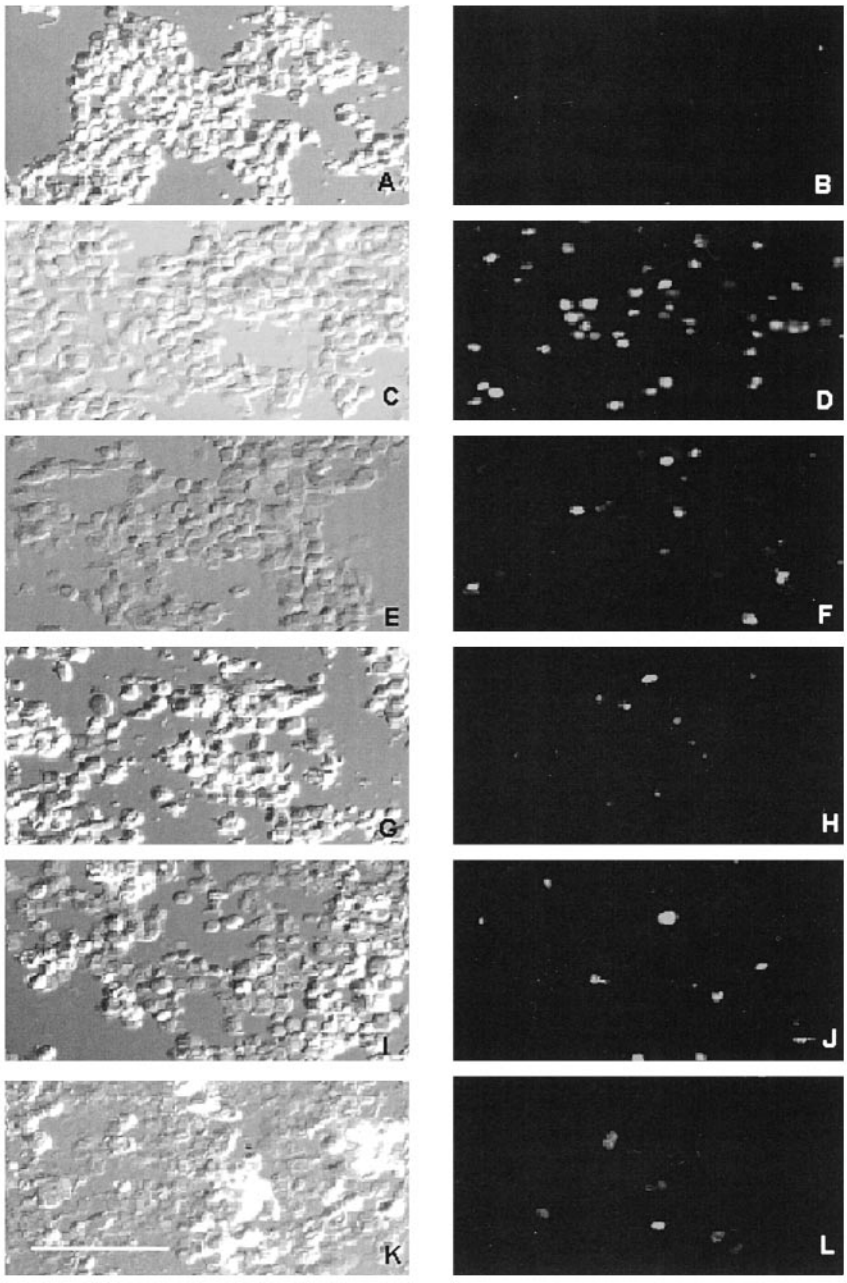

Fig. 5 Effect of TMZ on apoptosis in glial cell cultures. Immunocytochemical staining of apoptotic cells in mocked (*B*), SWB40 (*D*), SWB 95 (*F*), SWB 39 (*H*), D-54 (*J*), and SWB 77 (*L*) 48 h after treatment with 100 μM TMZ, respectively. *Left panels* show transmission image of the field shown on the *right*. Cells were grown in cover slides to 80% confluence, fixed, and stained for TUNEL as described in "Materials and Methods." Controls treated similarly but without primary antibody were run in parallel to ensure staining specificity. *Bar*, 100 μm.

DISCUSSION

The results presented here indicate that mechanisms of sensitivity and resistance to TMZ and presumably to other methylating agents is much more complex than the mechanism involved in the resistance to BCNU and other bifunctional alkylating agents. The low to moderate levels of MGMT found in the majority of human glial tumors do not effectively protect against TMZ, because TMZ alone is effective in suppressing such MGMT levels for up to 24 h.

The most effective mechanism of resistance of glial tumors to TMZ has been identified here as the loss of the p53-inducible cell cycle checkpoint. Apoptosis in glial tumors can be associated with a functional p53 cycle and correlates with a robust and extensive G_1-S cell cycle arrest in response to TMZ-induced damage. Tumors that had either a mutated p53 sequence or showed a sluggish response in mobilizing p21, exhibited higher levels of resistance than tumors with an active p53 response to DNA damage. With the exception of SWB77, which does not arrest in G_1-S after treatment with up to 200 μM TMZ, cell cycle arrest (in S phase) was observed in all of the treated cell lines regardless of expression of wt- or mut-p53, although the extent of the arrest correlated with p53 functional status being most

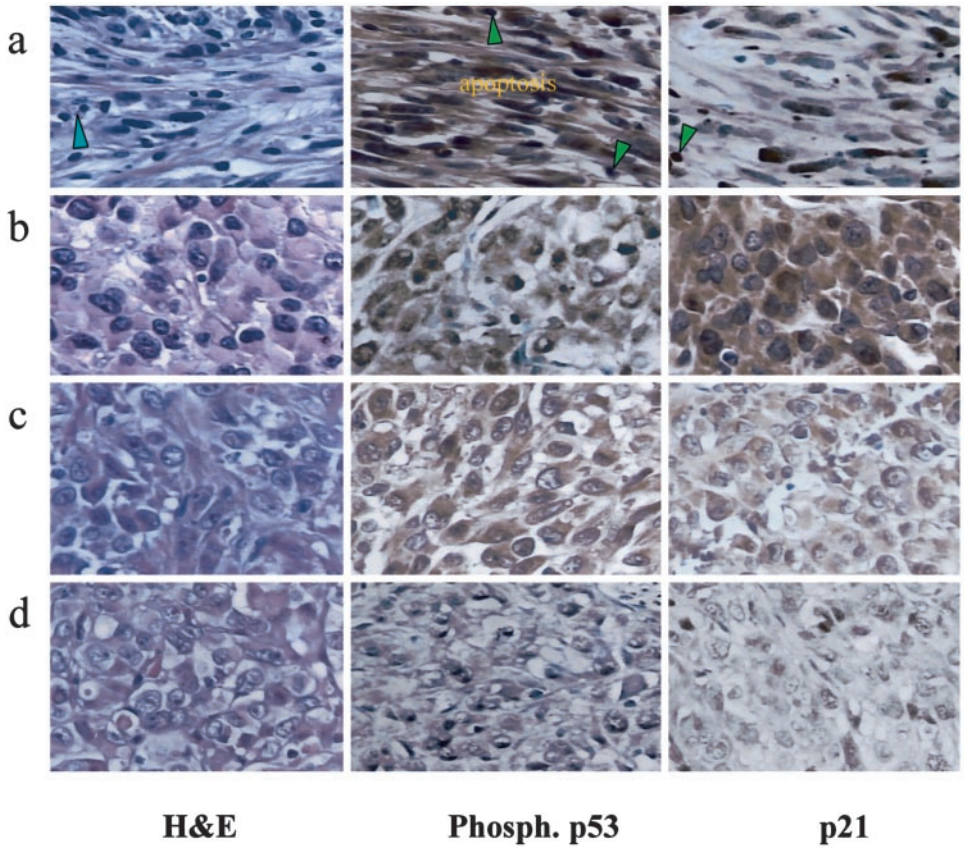

Fig. 6 Effect of TMZ on p53 phosphorylation, p53 translocation to the nucleus, and expression of p21 on glial tumor xenografts. Animals carrying glial tumor xenografts (350 + 25 mm^3) were treated with a single dose of TMZ (400 mg/m^2) and killed 24 and 48 h after treatment (five animals at each time point). Response to the drug as determined by expression of p21 and phosphorylated p53 was similar at these two time points, but apoptosis in responding tumor xenografts was more robust at 48 h after treatment. *Panels 1–4* correspond to SWB40, D-54, SWB77, and SWB95, respectively. *A*, *B*, and *C* are stained with H&E and for phosphorylated p53 and p21 plus methyl green counterstain, respectively. Note the robust expression of phosphorylated p53 and p21 in SWB40 (*B1* and *C1*, respectively) in the nuclei and the intense staining for p53 and p21 in apoptotic cells (*arrows*). Expression of p53 (nuclear) and p21 (cytoplasmic) is observed in D-54 (*B2* and *C2*) but to a much lesser extent than their respective expression in SWB40. Lack of expression of p53 and p21 in SWB77 in response to TMZ treatment (*B3* and *C3*) is in agreement with the absence of apoptotic cells (*A3*). Weak staining of cytosol for phosphorylated p53 is observed in SWB95 (*B4*), but there is no expression of p21 (*C4*). Original magnification ×400.

pronounced in wt-p53-expressing cells. Arrest in G_2/M phase was also observed only in mut-p53 cells and not in wt-p53 cells, which is in agreement with a previous report (20).

An additional mechanism of resistance to methylating agents is related to deficiencies in MMR repair (20, 30–32). Despite the expected toxicity by the action of MMR on unrepaired O^6-methyl G:T or C pairs, which are recognized by MSH2 or MLH1, glial tumor xenografts show variable resistance to methylating drugs that does not correlate with either their MGMT level nor with their MMR status. The failure of TMZ to yield a uniform response in the MMR-efficient glial tumor xenografts used in this study suggests that MMR is not the only factor determining the response of glial tumors to DNA-methylating drugs, and it may not even be the major one. Because MMR deficiency is thought to be low among glial tumors (33), factors that either limit capacity of MMR to kill cells carrying unrepaired mutations or even factors unrelated to such mechanism may determine the response of glial tumors to

Table 5 Apoptotic indices in glioma xenografts after treatment with TMZ

Xenograft treated	Time after TMZ (h)	Apoptotic index: untreated	TMZ
SWB77	24	4[a]	9 ± 4[b]
	48		11 ± 6
SWB95	24	3	33 ± 5
	48		64 ± 11
SWB33	24	6	22 ± 3
	48		21 ± 4
SWB40	24	7	28 ± 7
	48		34 ± 11
SWB61	24	7	44 ± 8
	48		61 ± 5
D-54	24	6	24 ± 4
	48		27 ± 5

[a] Apoptotic index in xenografts growing exponentially in athymic mice.

[b] Apoptotic index in xenografts after treatment with 400 mg/m^2 TMZ. Mean from three animals ±SD.

Table 6 Levels of MMR proteins in glioma xenografts

Cell line	MSH2	MLH1	PMS1
SWB77	1.0 ± 0.2[a]	0.5 ± 0.3	1.3 ± 0.3
SWB61	1.2 ± 0.1	0.8 ± 0.1	0.2 ± 0.1
SWB40	0.8 ± 0.1	0.5 ± 0.3	0.3 ± 0.1

[a] Relative band density; three determinations ±SD.

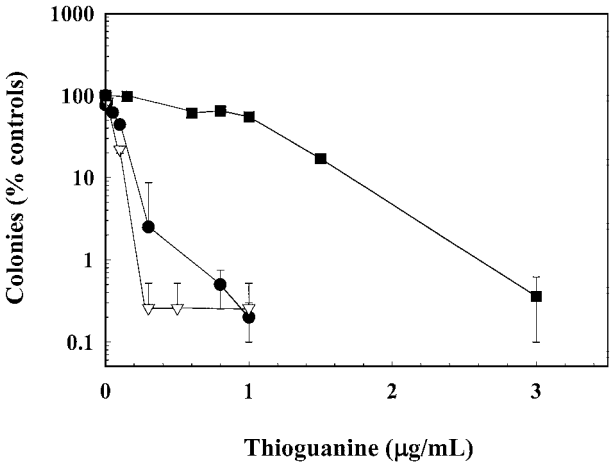

Fig. 7 TG toxicity for SWB77, SWB40, and the control MMR-deficient cell line LoVo (marked by ○, ■, ▽, respectively). The graph represents clonogenic efficiency with increasing concentrations of TG. Assays were set up as described in "Materials and Methods," and results are shown as number of colonies formed (as a percentage of the number of colonies in control plates); *bars*, ±SD. Assays were set up in quadruplicate and repeated in at least three independent runs.

chemotherapy or radiation in the clinic. That encourages additional search for understanding the limitations of MMR in tumors and also for seeking alternate pathways of tumor resistance to therapy.

The question of MGMT control by genes such as *p53*, which are already linked to the susceptibility of gliomas to treatment, clearly deserves additional investigation. For example, enforced expression of wt-p53 has been reported to curtail transcription of the *MGMT* gene in human tumor cells, thus enhancing their response to alkylating agents (34). Whether the ectopic expression of p53 modulates resistance to DNA damage by down-regulating MGMT or enhances the response of apoptotic pathways remains to be seen. Our results do not demonstrate a correlation between expression of wt-p53 and MGMT level in the glial tumors examined. Even more importantly, the response to TMZ as determined by apoptosis was entirely unrelated to MGMT levels regardless of the mutational status of p53. A direct involvement of MGMT in the response of gliomas to TMZ may apply in tumors expressing MGMT levels well above those of the xenografts used in this study (18), but such correlation does not seem applicable for the majority of glial tumors, which express MGMT levels below 100 fmol/mg protein.

Our data also demonstrate that the resistance of tumor cells that cannot repair O^6-methylguanine adducts because of their low MGMT expression appears not to be related to MMR status,

Table 7 Allelic loss resulting from treatment of glial tumor xenografts with BG and TMZ

Xenograft	Treatment	Total alleles	Informative alleles	Loss of heterozygosity	Clonal %[2]
SWB61	TMZ	13	4	1/4	20
SWB61	TMZ + BG	13	4	1/4	23
SWB40	TMZ	13	5	3/5	32
SWB40	TMZ + BG	13	5	4/5	65
D54	TMZ	13	4	3/4	55
SWB77	TMZ	13	5	5/5	99+
SWB77	TMZ + BG	13	5	5/5	99+

as it has been suggested previously (18). The MMR status of the cell lines used in this study was determined by the TG assay, which indicated similar efficiency of the overall mismatch-mediated repair in these lines. Microsatellite analysis after treatment of xenografts with BG and TMZ revealed that tumors regrown several weeks from treatment had a replication error negative phenotype, which also indicates MMR efficiency. Finally, Western analysis for MSH2 (which binds G-T mismatches), MLH1, which along with MSH2 defines the methylation-sensitive phenotype, and PMS1 showed high levels of expression and movement to the nucleus after DNA damage with TMZ. Although such analysis is extensive and convincing for a functional MMR system, it is still possible that methodologies applied here may not be sufficient to detect subtle differences in MMR response that could had defined the variable toxicity of the tumors to TMZ treatment.

The large extent of mutations allowed in SWB77 after treatment and regrowth implies that MMR does not always lead to cell death and that cells escaping the MMR-imposed cell cycle blocks may also escape scrutiny regarding the integrity of their genome. On the other hand, the lower incidence of mutations during regrowth of SWB40 and 61 indicates a much stricter control of mismatches by MMR, which may take place during p53-dependent lengthy cell cycle checkpoints imposed on these tumors after TMZ treatment. The differences in the extent of allelic loss between SWB61 and SWB77, the most responsive and most resistant gliomas to TMZ, respectively, can only result from differences in cell cycle responses to DNA damage and not from differences in the capacity to repair of O^6-methylguanine adducts, which would have predicted a more rapid repair in SWB77 than in SWB61. In fact, the capacity of glial xenografts to repair alkylation damage is severely restricted by the complete suppression of MGMT levels for at least 24 h after TMZ treatment or even 48 h after the combination of BG and TMZ. Overall, the present study demonstrates a limited MMR involvement in repair of glial tumors, which appear to possess highly functional MMR systems.

Although p53 status is useful in characterizing individual tumors and classes of tumors, our data indicate that at least for glial tumors mutated p53 is not always an accurate predictor of drug sensitivity and resistance. The fact that data are emerging to support both positive and negative correlations between p53 mutations and drug sensitivity supports our observation (35) and suggests a need to account for the discrepancies. Our data suggest that in brain tumors it is likely that cell cycle checkpoints, most notably those induced by a functional p53 response,

favor apoptosis and reduce the chance of mutations induced by methylating chemotherapeutic agents.

REFERENCES

1. Avgeropoulos, N. G., and Batchelor, T. T. New treatment strategies for malignant gliomas. Oncologist, *4:* 209–224, 1999.
2. Silbergeld, D. L., and Chicoine, M. R. Isolation and characterization of human malignant glioma cells from histologically normal brain. J. Neurosurg., *86:* 525–531, 1997.
3. Belanisch, M., Pastor, M., Randall, T., Guerra, D., Kibitel, J., Alas, L., Li, B., Citron, M., Wasserman, P., White, A., *et al*. Retrospective study of the correlation between DNA repair protein alkyltaransferase and survival of brain tumor patients treated with carmustine. Cancer Res., *56:* 783–788, 1996.
4. Jaeckle, K. A., Eyre, H. J., Townsend, J. J, Schulman, S., Knudson, H. M., Belanich, M., Yarosh, D. B., Bearman, S. I., Giroux, D. J., and Schold, S. C. Correlation of tumor O^6- methylguanine-DNA methyltransferase levels with survival of malignant astrocytoma patients treated with bis-chloroethylnitrosourea: A Southwest Oncology Group study. J. Clin. Oncol., *16:* 3310–3315, 1998.
5. Citron, M., Schoenhaus, M., Rothenberg, H., Kostroff, K., Wasserman, P., Kahn, L., White, A., Burns, G., Held, D., and Yarosh, D. O^6-Methylguanine-DNA methyltransferase in normal and malignant tissue of the breast. Cancer Investig., *12:* 605–610, 1994.
6. Kokkinakis, D. M., Ahmed, M., Delgado, R., Fruitwala, M., Mohiuddin, M., and Albores-Saavedra, J. Role of O6-methylguanine-DNA methyltransferase in the resistance of pancreatic tumors to alkylating agents. Cancer Res., *57:* 5360–5368, 1997.
7. Fischhaber, P. L., Gall, A. S., Duncan, J. A., and Hopkins, P. B. Direct demonstration in synthetic oligonucleotides that *N, N′*-Bis(2-chloroethyl)-nitrosourea cross-links N^1 of deoxyguanosine to N^3 of deoxycytidine on opposite strands of Duplex DNA[1]. Cancer Res., *59:* 4363–4368, 1999.
8. Karran, P., and Bignami, M. Self-destruction and tolerance in resistance of mammalian cells to alkylation damage. Nucleic Acids Res., *20:* 2933–2940, 1992.
9. Karran, P., and Hampson, R. Genomic instability and tolerance to alkylating agents. Cancer Surv., *28:* 69–85, 1996.
10. Schold, S. C., Kokkinakis, D. M., Rudy, J., Moschel, R. C., and Pegg, A. E. Treatment of human brain xenografts with O^6-benzyl-2′-deoxyguanosine and BCNU. Cancer Res., *56:* 2076–2081, 1996.
11. Friedman, H. S., Dolan, M. E., Pegg, A. E., Marcelli, S., Keir, S., Catino, J. J., Bigner, D. D., Schold, S. C., Jr. Activity of temozolomide in the treatment of central nervous system tumor xenografts. Cancer Res., *55:* 2853–2857, 1995.
12. Kokkinakis, D. M., Moschel, R. C., Pegg, A. E., and Schold, S. C. Eradication of human medulloblastoma tumor xenografts with a combination of O^6-benzyl-2′-deoxyguanosine and 1, 3-bis(2-hloroethyl)-1-nitrosourea. Clin. Cancer Res., *5:* 3676–3681, 1999.
13. Friedman, H. S., Kokkinakis, D. M., Luda, J., Friedman, A. H., Cokgor, I., Haglund, M. M., Ashley, D. M., Rich, J., Dolan, M. E., Pegg, A. E., Moschel, R. C., McLendon, R. E., Kerby, T., Herndon, J. E., Bigner, D. D., and Schold, S. C. Phase I trial of *06*-benzylguanine for patients undergoing surgery for malignant gliomas. J. Clin. Oncol., *16:* 3570–3575, 1998.
14. Friedman, H. S., Kerby, T., and Calvert, H. Temozolomide and treatment of malignant glioma. Clin. Cancer Res., *6:* 2585–2597, 2000.
15. Yung, W. K., Prados, M. D., Yaya-Tur, R., Rosenfeld, S. S., Brada, M., Friedman, H. S., Albright, R., Olson, J., Chang, S. M., O'Neill, A. M., Friedman, A. H., Bruner, J., Yue, N., and *et al*. Multicenter Phase II trial of Temozolomide in patients with anaplastic astrocytoma or anaplastic oligoastrocytoma at first relapse. J. Clin. Oncol., *17:* 2762–2771, 1999.
16. Harris, C. L., Remack, J. S., Houghton, P. J., and Brent, T. P. Wild type p53 suppresses transcription of the human O6-methylguanine-DNA methyltransferase gene. Cancer Res., *56:* 2029–2032, 1996.
17. Tentori, L., Lacal, P. M., Benincasa, E., Franco, D., Faraoni, I., Bonmassar, E., and Graziani, G. Role of wild-type p53 on the antineoplastic activity of TMZ alone of combined with inhibitors of poly(ADP-Ribose) polymerase. J. Pharmacol. Exp. Ther., *285:* 884–893, 1998.
18. Middlemas, D. S., Stewart, C. F., Kirstein, M. N., Poquette, C., Friedman, H. S., Houghton, P. J., and Brent, T. P. Biochemical correlates of TMZ sensitivity in pediatric solid tumor xenograft models. Clin. Cancer Res., *6:* 998–1007, 2000.
19. Walker, D. R., Bond, J. P., Tarone, R. E., Harris, C. C., Makalowski, W., Boguski, M. S., and Greenblatt, M. S. Evolutionary conservation and somatic mutation hotspot maps of p53: correlation with p53 protein structural and functional features. Oncogene, *19:* 211–218, 1999.
20. D'Atri, S., Tentori, L., Lacal, P. M., Graziani, G., Pagani, E., Benincasa, E., Zambruno, G., Bonmassar, E., and Jiricny, J. Involvement of the mismatch repair system in TMZ-induced apoptosis. Mol. Pharmacol., *54:* 334–341, 1998.
21. Hainaut, P., and Hollstein, M. P53 and human cancer: the first ten thousand mutations. Adv. Cancer Res., *77:* 81–137, 2000.
22. Ferreira, C. G., Tolis, C., and Giaccone, G. p53 and chemosensitivity. Ann. Oncol., *10:* 1011–1021, 1999.
23. El-Deiry, W. Regulation of p53 downstream genes. Semin. Cancer Biol., *8:* 345–357, 1998.
24. Kokkinakis, D. M., Hoffman, R. M., Frenkel, E. P., Wick, J. B., Han, Q., Xu, M., and Schold, S. C. Synergy between methionine stress and chemotherapy in the treatment of brain tumor xenografts in athymic mice. Cancer Res., *61:* 4017–4023, 2001.
25. Robins, M. J., Khwaja, T. A., and Robins, R. K. Purine nucleosides: XXIX. The synthesis of 2′-deoxy-L-adenosine and 2′-deoxy-L-guanosine and their α-anomers. J. Org. Chem., *35:* 636–639, 1970.
26. Pauly, G. T., Powers, M., Pei, G. K., and Moschel, R. C. Synthesis and properties of H-ras DNA sequences containing O^6-substituted-2′-deoxyguanosine residues at first, second, or both positions of codon 12. Chem. Res. Toxicol., *1:* 391–397, 1988.
27. Kokkinakis, D. M., Von Wronski, M. A., Vuong, T. H., Brent, T. P., and Schold, S. C., Jr. Downregulation of O^6- methylguanine-DNA alkytransferase and sensitization of human tumor cell lines to nitrosoureas by methionine deprivation. Br. J. Cancer, *75:* 779–788, 1997.
28. Hawk, C. T., and Leary, S. L., Formulatory for Laboratory Animals, p. 78. Ames, IA: Iowa State University Press, 1995.
29. Horton, J. K., Roy, G., Piper, J. T., Awasthi, C. Y., Alaoui-Jamali, M. A., Boldogh, I., and Singhal, S. S. Characterization of a chlorambucil-resistant human ovarian carcinoma cell line overexpressing glutathione S-transferase μ. Biochem. Pharmacol., *58:* 693–702, 1999.
30. Kokkinakis, D. M., Bocangel, D. B., Schold, S. C., Moschel, R. C., and Pegg, A. E. Thresholds of O^6-alkylguanine-DNA alkyltransferase which confer significant resistance of human glial tumor xenografts to treatment with 1, 3-bis(2-chloroethyl)-1-nitrosourea or temozolomide. Clin. Cancer Res., *7:* 421–428, 2001.
31. Friedman, H., McLendon, R. E., Kerby, T., Dugan, M., Bigner, S. H., Henry, A. J., Ashley, D. M., Krischer, J., Lovell, S., Rasheed, K., Marchev, F., Seman, A. J., Cokgor, I., Rich, J., Stewart, E., Colvin, O. M., Provenzale, J. M., Bigner, D. D., Haglund, M. M., Friedman, A. H., and Modrich, P. L. DNA mismatch repair and O^6-alkylguanine-DNA alkyltransferase analysis and response to Temodal in newly diagnosed malignant gliomas. J. Clin. Oncol., *16:* 3851–3857, 1998.
32. Christmann, M., and Kaina, B. Nuclear translocation of mismatch repair proteins MSH2 and MSH6 as a response of cells to alkylating agents. J. Biol. Chem., *275:* 36256–36262, 2000.
33. Silber, J. R., Bobola, M. S., Ghatan, S., Blank, A., Kolstoe, D. D., and Berger, M. S. O6-Methylguanine-DNA methyltransferase activity in adult gliomas: relation to patient and tumor characteristics. Cancer Res., *58:* 1068–1073, 1998.
34. Srivenugopal, K. S., Shou, J., Mullapundi, S. R. S., Lang, Jr., F. F., Jasti, S. R., and Ali-Osman, F. Enforced expression of wild-type p53 curtails the transcription of the O(6)-methylguanine-DNA methyltransferase gene in human tumor cells and enhances their sensitivity to alkylating agents. Clin. Cancer Res., *7:* 1398–409, 2001.
35. Hirose, Y., Berger, M. S., and Pieper, R. O. Abrogation of the Chek1-mediated G_2 checkpoint pathway potentiates TMZ-induced toxicity in a p53-independent manner in human glioblastoma cells. Cancer Res., *61:* 5843–5849, 2001.

Clinical Cancer Research

Multifaceted Resistance of Gliomas to Temozolomide

Dora B. Bocangel, Sydney Finkelstein, S. Clifford Schold, et al.

Clin Cancer Res 2002;8:2725-2734.